

Identification of sweet spots in shale reservoir formations

Ritesh Kumar Sharma¹ and Satinder Chopra¹

Abstract

The main goal for shale resource characterization is usually the identification of sweet spots which represent the most favourable drilling targets. Such sweet spots can be picked up as those pockets in the target formation that exhibit high total organic carbon (TOC) content as well as high brittleness. At any well location, when the resistivity and sonic transit-time curves are scaled and overlaid, they follow each other almost everywhere, except in the kerogen-rich zones, where they cross over. While such a cross over is only seen visually, it can be transformed into an attribute known as $\Delta\log R$ that incorporates both the resistivity and velocity information and is expected to be high for organic-rich zones. Such a transformation would allow us to identify organic-rich zones only at well locations. In this study, we introduce a methodology for computing $\Delta\log R$ as a volume from seismic data. For doing this, the $\Delta\log R$ curve computed at well locations is correlated with different attribute curves that can be derived from seismic data. An attribute curve which shows the maximum correlation is selected and crossplotted against $\Delta\log R$ to determine the relationship between the two. This relationship is then used for extracting the $\Delta\log R$ volume from 3D seismic data.

Introduction

Although conventional reservoirs remain a very important part of the world's oil and natural gas supply, horizontal drilling and multi-stage fracturing have now made it possible to develop and exploit unconventional reservoirs. Regional and thick shale reservoir rock formations are usually preferred for their economic exploitation. However, their physical properties vary in the vertical and horizontal directions. Of the many properties, maturation, mineralogy, pore pressure, organic richness, permeability, brittleness and gas-in-place are some of the key elements of a successful shale resource play (Chopra et al., 2012). Maturation and mineralogy are usually determined from geochemical analysis of the rock samples and are difficult to derive from seismic data. The organic richness of a shale formation is associated with the total organic carbon (TOC) content. Thus the computation of TOC volume from seismic data would allow the lateral mapping of organic content in a shale formation. We attempt to identify the sweet spots with the application of Passey et al.'s (1990) approach to seismic data.

For detecting organic-rich depth intervals in shale zones at the well locations, Passey et al. (1990) proposed a technique based on sonic and resistivity curves overlay. The transit time and resistivity curves are scaled in such a way that the two curves overlay each other. However, in the organic-rich intervals the two curves exhibit a crossover, which is a good indication. This crossover can be defined in

terms of $\Delta\log R$ which is computed from log data using the equation:

$$\Delta\log R = \log\left(\frac{rt}{rt_{baseline}}\right) + 0.02(dt - dt_{baseline}), \quad (1)$$

where rt is the resistivity, dt is the sonic transit time and $rt_{baseline}$, $dt_{baseline}$ are resistivity and sonic values corresponding to the overlapping zone. For organic rich zones where sonic and resistivity curves yields a crossover, $\Delta\log R$ is expected to be high as shown in Figure 1. Passey et al. (1990) also discuss similar empirical equations for density and neutron porosity, which may as well exhibit linear relationships with TOC, but usually greater scattering of points is observed on the crossplots for these variables. For this reason, it is quite common to see the application of the empirical equation between $\Delta\log R$, resistivity and sonic logs.

Once $\Delta\log R$ is known, TOC can be computed by using the following equation:

$$TOC = \Delta\log R * 10^{(2.297 - 0.1688 * LOM)} \quad (2)$$

Here, it is noticed that TOC is a function of $\Delta\log R$ and LOM (level of maturity). While $\Delta\log R$ can be computed using well-log data, LOM is rarely known. However its range of variation is documented (Passey et al., 1990) and known to vary between 7 and 14. We crossplotted TOC with $\Delta\log R$ using different values of LOM. Such a crossplot

¹ Arcis Seismic Solutions, TGS, Calgary, Canada.

* Corresponding author, E-mail: schopra@arcis.com

reveals a linear relationship regardless of the LOM value, and is shown in Figure 2. It can be concluded here that in the absence of LOM, $\Delta\log R$ can be useful for obtaining TOC information in a qualitative way.

Thus, we extend Passey et al.'s. (1990) approach with its application to seismic data. For doing this we first compute $\Delta\log R$ attribute from log data by using the equation mentioned above. Next we crossplot this curve with other attributes that can be computed from seismic data. That attribute pair which shows the best correlation is picked up and the relationship between them is determined. This relationship is then used to determine the $\Delta\log R$ volume from seismic data. The complete workflow adopted in this study is shown in Figure 3.

Application to Duvernay play

The Duvernay shale liquids play running along the foothills east of the Rocky Mountains, possesses all the prerequisites of being a successful unconventional play, and has gained the attention of the oil and gas industry in Alberta, Canada. The Duvernay shale play has been recognized as the source rock for many of the large Devonian oil and gas pools in Alberta, including the early discoveries of conventional

hydrocarbons near Leduc. The Duvernay shale basin spans approximately 50,000 square miles, with an estimated 7500 square miles within the thermally mature or wet gas window (Davis and Karlen, 2013) from northwest to southeast across Alberta. Its stratigraphic age is equivalent to the Muskwa Formation of the Horn River dry shale gas play to the northwest in the neighboring province of British Columbia (Rivard et al., 2013).

The Duvernay was deposited in a broad marine setting as a basin-filling shale surrounded by equivalent aged Leduc reef build-ups. Owing to rapid basin filling during maximum sea-level transgressions, enormous quantities of organic sediments were dumped in this deep, oxygen-starved basin that are the present day Duvernay source rocks, where TOC (total organic carbon) is as high as 20% (McMillan et al., 2014). The Duvernay shale is fine-grained and silica rich. As a result of the fine grains, rocks have increased total surface area that leads to a higher absorbed gas component in organic-rich rocks. Moreover, silica-rich rocks are more brittle and favorable for fracking. It is also known that the Duvernay formation is overpressured that leads to better storage of hydrocarbons. For these reasons the Duvernay shale is considered as an emerging shale liquids play in Canada.

As stated earlier, the Duvernay Formation is an Upper Devonian source rock that covers a significant part of west-central Alberta of the Western Canadian Sedimentary Basin (WCSB), as shown in the index map in Figure 4 (Rokosh et al., 2012). In Alberta, the Duvernay shales are found in the East shale basin and West shale basin, both of which differ in the geological setting and their characteristics. The present study focuses on a dataset from central Alberta and situated in the West Shale Basin.

In order to characterize the Duvernay formation based on its organic richness, we first compute $\Delta\log R$ curve from log data and crossplot this curve with other attributes that can be computed from seismic data. Examples of such attributes are (V_p/V_s) ratio, Poisson's ratio, λ/μ (where λ

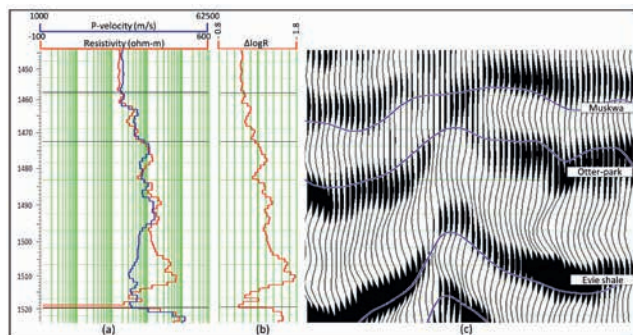


Figure 1 (a) Resistivity and sonic curves overlaid according to Passey et al.'s. (1990) method showing the crossover for organic-rich interval. (b) $\Delta\log R$ curve computed using Passey's approach is high for that interval. (c) Segment of a seismic section with the horizons in the zone of interest overlaid, shown correlated with the log curves.

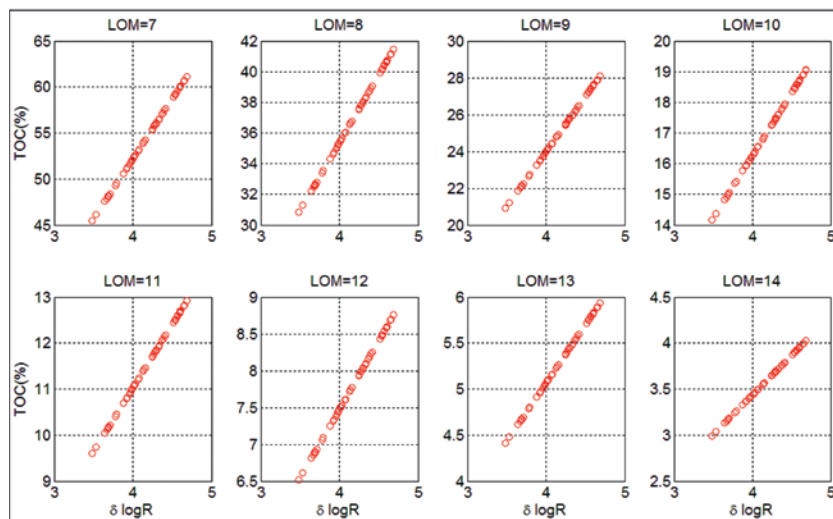


Figure 2 Crossplot of TOC versus $\Delta\log R$ using different values of LOM over a known range. A linear relationship is seen between TOC and $\Delta\log R$ regardless of the LOM value.

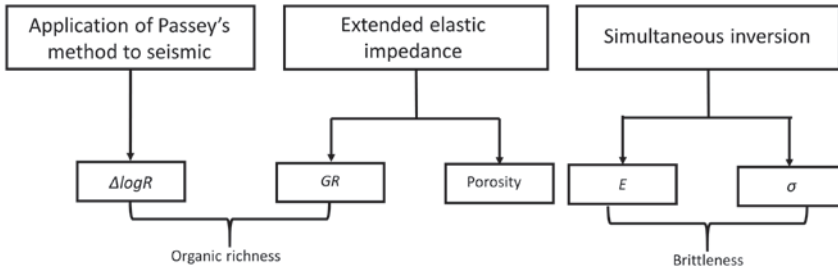


Figure 3 Workflow for identification of sweet spots in shale reservoir formations.

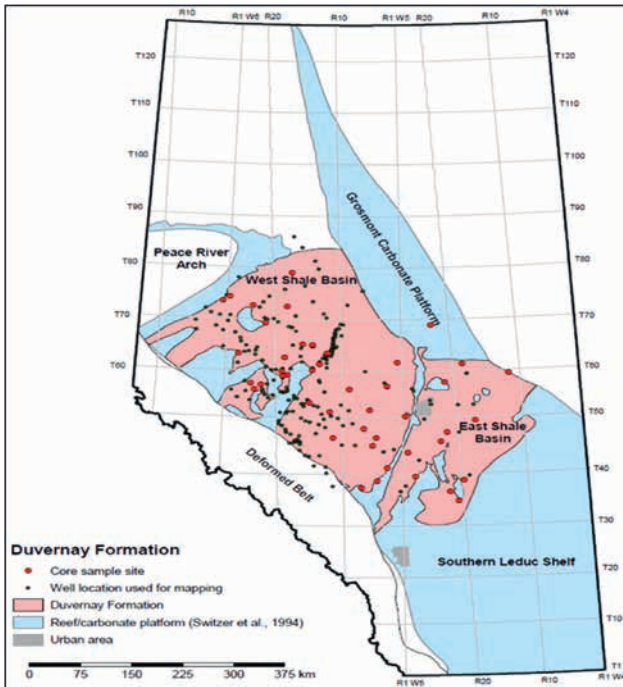


Figure 4 Index map showing the Duvernay Formation in the province of Alberta (After Rokosh et al., 2012).

and μ are Lamé' parameters), Poisson's impedance, Poisson damping factor and some others. Poisson impedance was introduced by Quakenbush et al. (2006) as $PI = AI - cSI$, and describes a rotation of the data in $AI-SI$ crossplot space to obtain litho-fluid discrimination. In this equation, AI is acoustic impedance and SI is shear impedance and the index 'c' optimizes this rotation. Poisson damping factor attribute discriminates lithological variations, e.g. the pay sandstones from the shale, and also shows variation in sandstone quality. In Figure 5 we show four such crossplots. We notice that the cluster points are seen scattered on three of the four crossplots, the exception being the $\Delta\log R$ versus $[\lambda\rho / (\lambda\rho + 2\mu\rho)]$ attribute crossplot. This crossplot shows a good linear relationship between the two attributes with a correlation coefficient of 87%. We determine this relationship from the crossplot which can be used to transform the $[\lambda\rho / (\lambda\rho + 2\mu\rho)]$ derived from seismic data to $\Delta\log R$ volume. As it is known that $\lambda\rho$ and $\mu\rho$ are function of P- and S-impedances, we have followed an updated workflow of simultaneous inversion proposed by authors (Sharma and Chopra, 2013). As per this workflow, after generating

angle gathers from the conditioned offset gathers, Fatti's approximation to Zoeppritz equations (Fatti et al., 1994) is used to compute P-reflectivity (R_p) and S-reflectivity (R_s). The density attribute could not be extracted as the seismic data was not acquired with long offsets. Once reflectivities were extracted, thin-bed reflectivity inversion was performed on each individually. The reason for running thin-bed reflectivity inversion is owing to the fact that the Upper Duvernay formation being considered in this case study is not thick enough throughout and for most of the survey falls below typical seismic resolution. Thus a method to enhance the resolution of the seismic data is needed as part of the workflow. The method of choice for us was the thin-bed reflectivity inversion that has been described and illustrated elsewhere (Chopra et al., 2006, 2009; Puryear and Castagna, 2008).

In this process, the time-varying effect of the wavelet is removed from the data and the output of the inversion process can be viewed as spectrally-broadened seismic data, retrieved in the form of broadband reflectivity which can be filtered back to any desired bandwidth. This usually represents useful information for interpretation purposes. Filtered thin-bed reflectivity, obtained by convolving the reflectivity with a wavelet of a known frequency band-pass, not only provides an opportunity to study reflection character associated with features of interest, but also serves to confirm its close match with the original data.

Thin-bed reflectivity inversion is a poststack process and rather than using simultaneous inversion in our workflow, we modified it by including the application of Fatti's approximation to Zoeppritz equations (Fatti et al., 1994) and extracting P-reflectivity, S-reflectivity and density-reflectivity (which depends on the data quality) from the angle gathers. Once these reflectivities were obtained, thin-bed reflectivity inversion was run on each individually. In Figure 6 we show a comparison of the filtered thin-bed reflectivity inversion with the P-reflectivity seismic data. Additional reflection event cycles are present in the zone of interest (ZOI), and the overlaid impedance logs confirmed that the additional events were genuine. Next, a well-tie analysis was performed using the filtered P-wave reflectivity with a broader bandwidth than the input seismic, and is shown in Figure 7. On comparison it is noted that additional events created by the thin-bed

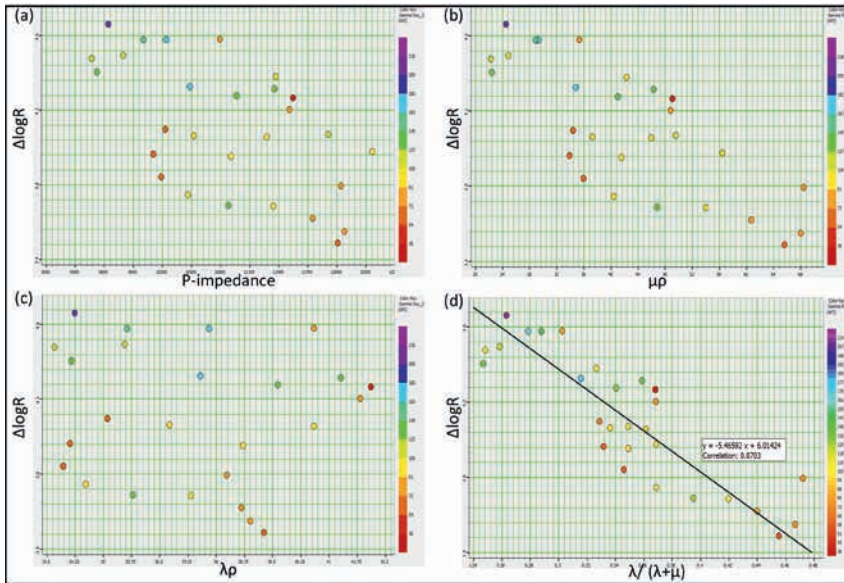


Figure 5 Crossplots of $\Delta\log R$ with (a) IP (b) $\mu\rho$, (c) $\lambda\rho$, and (d) $\lambda/(\lambda+2\mu)$ ratio. Scattering of cluster points and lower correlation is noticed for all the cases except $\lambda/(\lambda+2\mu)$, where a correlation of 87% is seen. The equation corresponding to linear relationship is obtained and used for obtaining $\Delta\log R$ volume.

reflectivity inversion match fairly well with the well data, and therefore could be trusted. Having gained the confidence in the frequency enhancement of R_p and R_s , these reflectivities were filtered and inverted into P- and S- impedances, individually, using post-stack model-based inversion. Once the impedances were extracted, the ratio $[\lambda\rho/(\lambda\rho+2\mu\rho)]$ volume was computed. This volume was then transformed into $\Delta\log R$ volume using the relationship shown on Figure 4d. As we desire to identify organic richness in a lateral sense over the interval of interest on a 3D volume we generate horizon slice of $\Delta\log R$ over a 10ms window (see Figure 8). We interpret high $\Delta\log R$ values as corresponding to organic rich zones, and are shown enclosed within a black outline. With this done, we have used a blind well to confirm it. Figure 9a shows the comparison of inverted $\Delta\log R$ (blue curve) and measured TOC from core data (red curve) for a blind well. The match is seen to be good as the increasing and decreasing trends seem to follow each other. A crossplot between TOC and $\Delta\log R$ is shown in Figure 9b. A correlation of 90% is noticed which again lends confidence to the analysis. Such a qualitative analysis can be transformed now into quantitative analysis by obtaining TOC volume from $\Delta\log R$

volume using the relationship between these two shown on Figure 9b.

Application to Montney play

The Montney play is one of the active natural gas plays in North America. The Montney is a thick and regionally charged formation of unconventional tight gas distributed in an area extending from north central Alberta to north-west British Columbia, Canada. The primary focus is the Lower and Upper Montney units for horizontal drilling, and we would expect that the Montney formation to exhibit high values of porosity, resistivity, gamma ray, and brittleness for being a prospective shale reservoir rock. We begin with Passey et al.'s. (1990) method at the well location and overlay the resistivity and sonic curves covering the Montney formation to identify the source rock. Identifying the crossover between these curves in the Upper Montney (UM) zone as shown in Figure 10, we conclude that that interval is the potential reservoir rock. With this known at the well location, we would like to map it laterally within this interval. For doing so we first compute $\Delta\log R$ curve from log data and crossplot this curve with other attributes that can be computed from seismic data.

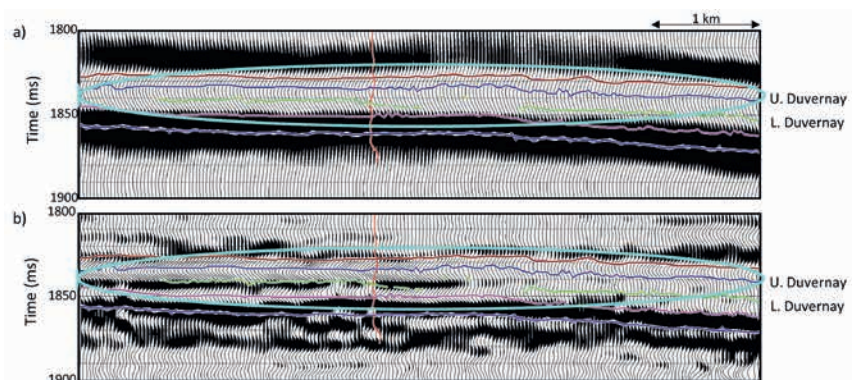


Figure 6 P-wave reflectivity section (a) before and (b) after thin-bed reflectivity process. Notice the extra events and more detailed information over the zone of interest highlighted by the light blue ellipses.

Figure 7 Well to seismic tie with the filtered P-wave reflectivity. Correlation of extra events in the ZOI provide the confidence in frequency enhancement.

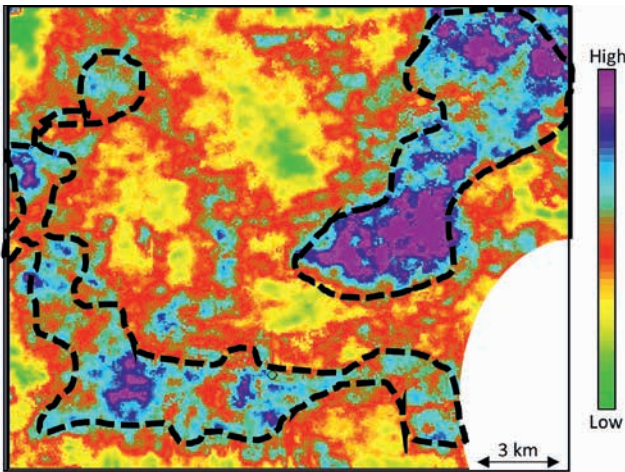
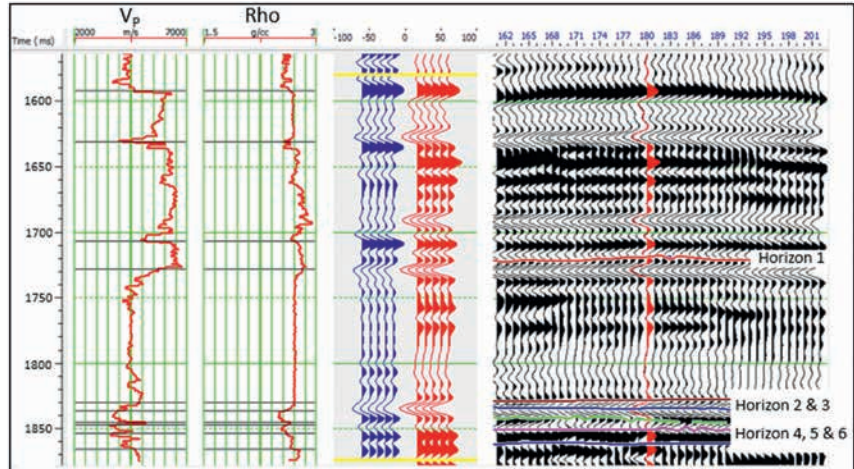


Figure 8 Horizon slice from the $\Delta\log R$ volume 10ms interval below the Duvernavy top marker. Notice the trend we see for high values of $\Delta\log R$ is not very different from what we see on the constrained volume display shown alongside.

In Figure 11 we show four such crossplots. We notice that the cluster points are seen scattered on three of the four crossplots, the exception being the $\Delta\log R$ versus $\lambda\rho$ attribute crossplot. This crossplot shows a good linear

relationship between the two attributes with a correlation coefficient of 94%. We determine this relationship from the crossplot and later use it to transform the $\lambda\rho$ derived from seismic data to $\Delta\log R$ volume. As P- and S-impedances are required for obtaining $\lambda\rho$, simultaneous inversion, which facilitates the estimation of these, was adopted. Figure 12a shows the horizon slice of $\Delta\log R$ over a 10ms window within the zone of interest. Shale reservoir rock indicative of high $\Delta\log R$ is seen mapped by black outline.

In the absence of core samples for this study we have computed other properties that are prerequisites for a shale reservoir rock. Porosity, gamma ray (GR) and brittleness are other properties that are of interest for characterizing shale formations. These conclusions are based on the fact that the higher the porosity, the better the reservoir quality. Furthermore, there is evidence of a linear relationship between the uranium content in shale and its organic content (Mendelson and Toksoz, 1985), though exceptions may exist (Lüning and Kolonic, 2003). Consequently, though a large gamma ray response is seen for shale formations, but the uranium spectral gamma ray curves correlate better with the presence of organic content in the rock intervals. Thus the computation of GR and porosity volumes from

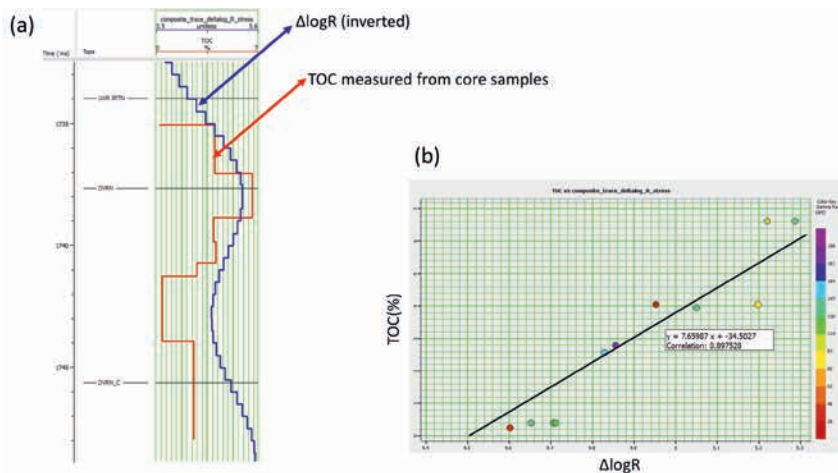


Figure 9 (a) The TOC values obtained from measurements on core samples over the zone of interest are shown in the form of a curve (red). This was a blind well test. Overlaid on this curve is the $\Delta\log R$ curve (blue) obtained by inversion of the seismic data. The match is seen as good as the increasing and decreasing trends seem to follow each other; (b) a crossplot between TOC and $\Delta\log R$ shows a correlation of 90%, which again lends confidence to the analysis.

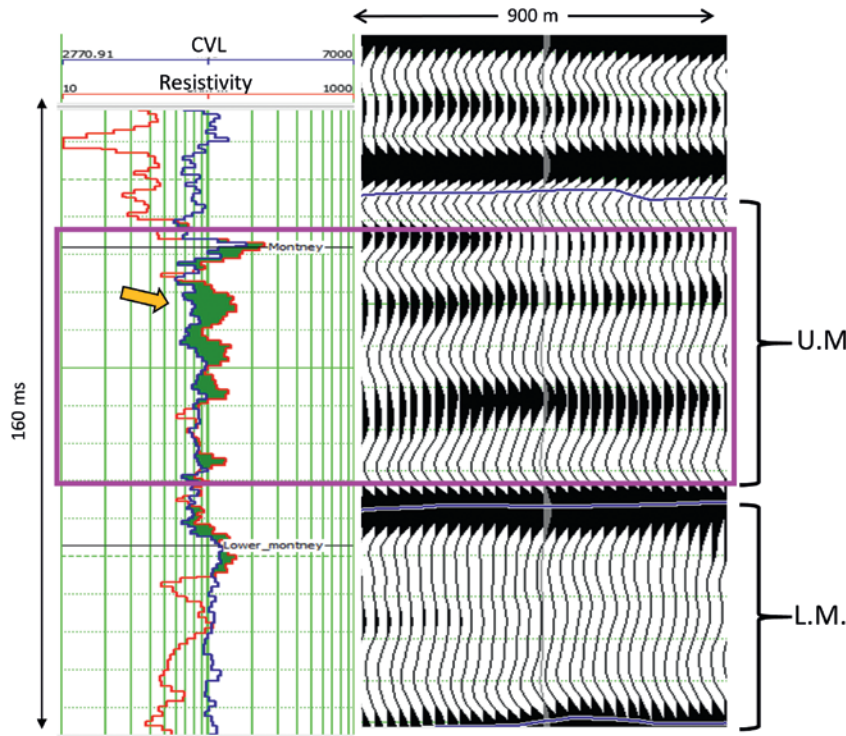


Figure 10 Resistivity and sonic curves overlaid as per Passey et al. (1990). The Upper Montney zone enclosed in the magenta box shows the characteristics of a hydrocarbon-bearing formation. The yellow block arrow indicates the narrow zone that is most prospective.

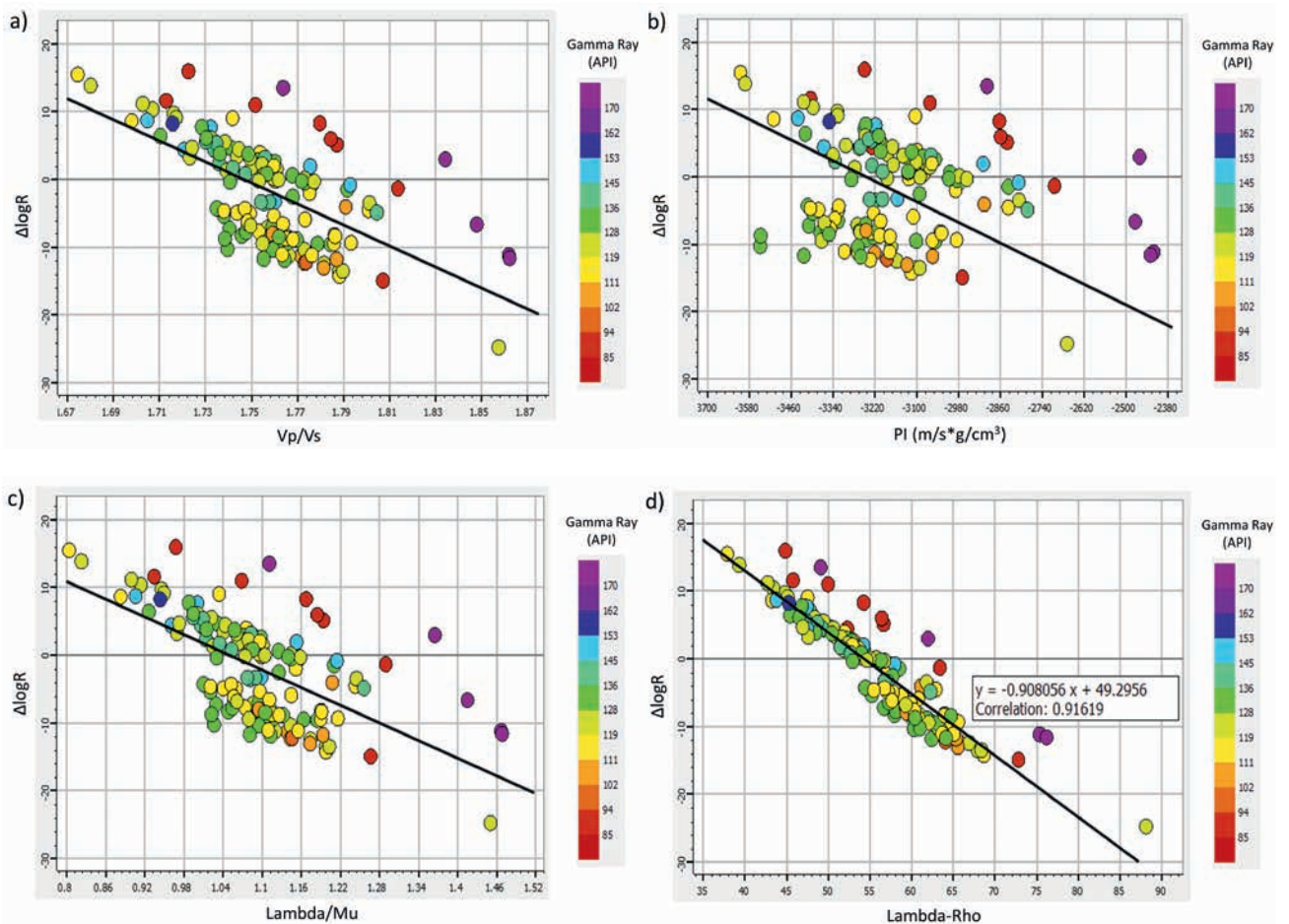


Figure 11 Crossplots of $\Delta\log R$ with (a) V_p/V_s , (b) PI , (c) λ/μ and (d) $\lambda\rho$. Scattering of cluster points and lower correlation is noticed in all cases except $\lambda\rho$, where a correlation of 92% is observed. The equation corresponding to the observed linear relationship is obtained and used for obtaining $\Delta\log R$ volume.

Figure 12 Horizon slices from (a) $\Delta\log R$ (b) Poisson's ratio (c) porosity, and (d) Young's modulus. Shale reservoir rock indicative of high $\Delta\log R$, low PR, high YM is seen mapped by black polygons.

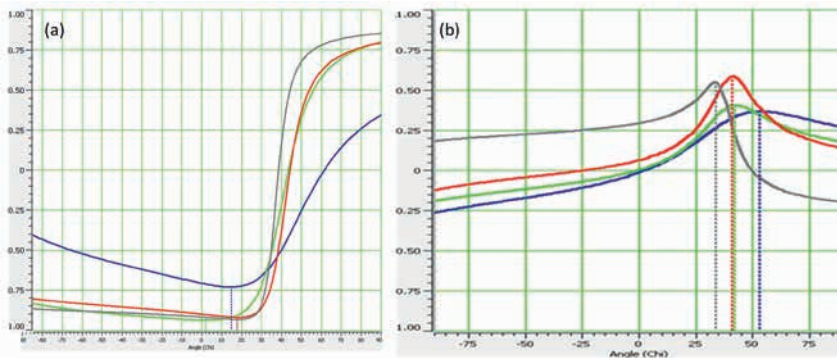
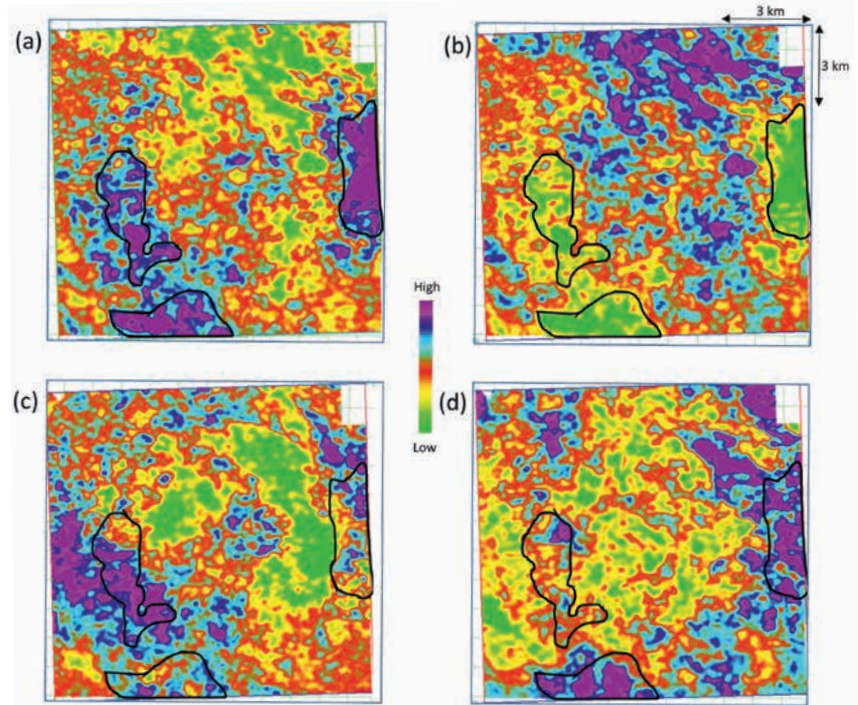


Figure 13 (a) Correlation between EEI logs and (a) porosity curves (b) GR curves, for four different wells. For porosity the maximum negative correlation occurs at 18 degrees for the red curve. For GR, the maximum positive correlation occurs at 42 degrees again for the red curve.

seismic data would allow the lateral mapping of organic content in a shale formation. As stated earlier, brittle rocks fracture much better than ductile rocks and enhance their permeability, so shale reservoir rocks must exhibit high brittleness if optimum production has to be sought from them. Such information can be extracted from the seismic data through Young's modulus (E) or $E\rho$ (product of Young's modulus and density) and Poisson's ratio (Sharma and Chopra, 2015).

Elastic impedance inversion (EEI) is a generalization of acoustic impedance for variable angle of incidence, and provides a consistent and absolute framework to calibrate and invert non-zero offset seismic data (Connolly, 1999) for fluid discrimination and lithology prediction for reservoirs. However, the elastic impedance values decrease with increasing angle of incidence and require a scale factor of varying angles if it were to be compared to the acoustic impedance. Whitcombe (2002) not only introduced normalizing constants to remove the variable dimensionality and overcame this problem, but also introduced extended elastic

impedance (EEI) (Whitcombe et al., 2002), which broadens the definition of elastic impedance. As per this formulation, some of the rock properties cannot be predicted by the elastic impedance approach that usually considers the angle of incidence range as 0 to 30°, which are the values taken by $\sin^2\theta$. Consequently, by bringing about a change of variable, i. e. $\sin^2\theta$ replaced with $\tan\chi$ the angle range is extended from -90° to +90° and this allows calculation of impedance value beyond the physically observable range of angle θ . The χ angle can be selected to optimize the correlation of the EEI curves with petrophysical reservoir parameters, such as V-shale, water-saturation and porosity or with elastic parameters such as bulk modulus, shear modulus and Lamé constant and so on.

The extended elastic impedance (EEI) approach (Whitcombe et al., 2002) was adopted for obtaining GR and porosity volumes from seismic data. To execute this approach, the first step is the correlation analysis between EEI logs and available petrophysical logs (porosity and gamma ray). Such a correlation of EEI log with porosity

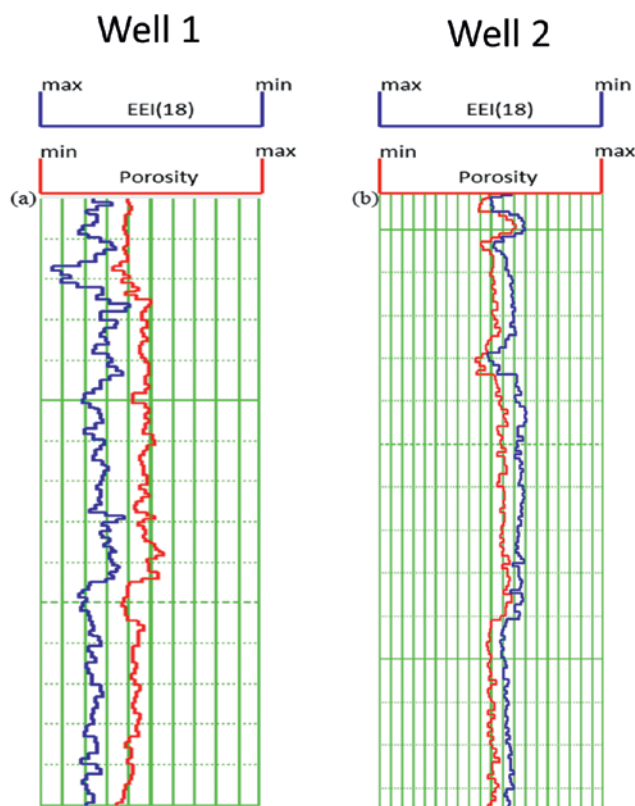


Figure 14 Comparison of EEI log computed at 18° (angle corresponding to maximum correlation shown in Figure 3a) with the measured porosity curve at (a) well 1 and (b) well 2. The resemblance between both sets of curves is striking.

and GR for various angles is shown in Figure 13a and 13b respectively. Four wells data are included for this analysis. For porosity, though all the wells show a negative minima over a range of angles 2 to 18° , two wells (red and grey curves) show a maximum correlation of 92% at 18° angle. This angle was then used for computing EEI log that resembles the porosity curves at the well locations (Figure 14). Such a good correlation seen on the predicted porosity and the actual measured porosity curves lends confidence to the analysis being carried out. A similar observation was made for the GR curves. Having known these angles, equivalent seismic data volumes are generated using intercept and gradient volumes computed from angle gathers and inverted into porosity and GR volumes using post-stack model based inversion.

The next step was to determine the brittleness information, as pockets with high brittleness fracture better and will serve as sweet spots for our characterization. Simultaneous inversion was adopted for obtaining this information, which yielded P-impedance, S-impedance as well as density. The computation of density was possible as far-offset range was available in the data. Using these attributes Young's modulus (YM) and Poisson's ratio (PR) were determined. Having 3D volumes of these attributes, we generated horizon slices for Poisson's ratio, porosity

and Young's modulus and are shown in Figure 12b, c and d. We interpreted high $\Delta\log R$, YM, porosity and low PR values corresponding to the organic-rich zone within the Upper Montney zone. These are shown mapped by black polygons.

Conclusions

Considering the fact that Duvernay and Montney Formations are the emerging unconventional shale plays in Canada, an attempt was made to characterize them using seismic data from the study area in central Alberta. Understanding the importance of organic richness for identifying the sweet spots in an unconventional play, a new approach was proposed to obtain TOC information in a lateral sense over the interval of interest by making use of Passey's method. At the well locations Passey et al.'s (1990) method indicates that Upper Duvernay and Upper Montney show the characteristics of the reservoir rock, as $\Delta\log R$ showed high values. Subsequently, using crossplotting between different attributes and $\Delta\log R$, it was found that while $\lambda\rho/(\lambda\rho+2\mu\rho)$ attribute showed the high correlation (87%) for the Duvernay Formation, the highest correlation (94%) for the Montney Formation was shown by $\lambda\rho$ attribute. Thus, we concluded that the maximum correlation of seismically derived attribute with $\Delta\log R$ is data dependent. The linear relationship between seismically derived attribute that yields maximum correlation and $\Delta\log R$ was used to transform that seismically derived attribute volume into a $\Delta\log R$ volume. Organic-rich zones were identified adopting the criteria of high $\Delta\log R$. Blind well analysis was followed up to obtain the confidence in the proposed approach. For a blind well over the Duvernay Formation, a correlation of 90% was noticed between TOC measured from core samples and $\Delta\log R$ which lent confidence to the analysis. In the absence of core data for the Montney formation, porosity, GR and brittleness information for characterizing shale reservoir rocks were derived by considering their importance along with the organic richness information. Finally, sweet spots were identified adopting the criteria of low Poisson's ratio, high $\Delta\log R$, high porosity, and high Young's modulus. As the developed methodology has demonstrated its importance for characterizing Duvernay and Montney Formations, we recommend its application for characterization of other shale plays.

Acknowledgements

We thank an anonymous company for generously providing permission for the data examples in the first case study. We also thank Arcis Seismic Solutions, TGS, for allowing us to present this work.

References

- Chopra, S., R. K. Sharma, J. Keay and K. J. Marfurt, [2012] Shale gas reservoir characterization workflows: 82nd Annual International Meeting, SEG, Expanded Abstracts, 1-5.

- Chopra, S., J. P. Castagna, and O. Portniaguine, [2006] Seismic resolution and thin-bed reflectivity inversion, *CSEG Recorder*, **31**, 19–25.
- Chopra, S., J.P. Castagna and Y. Xu, [2009] Thin-bed reflectivity inversion and some applications, *First Break*, **27**, 27–34.
- Davis, M., and G. Karlen, [2013] A Regional Assessment of the Duvernay Formation; a World Class-Liquids Rich Shale Play, *CSEG GeoConvention*, Expanded Abstracts.
- Fatti, J. L., P. J. Vail, G. C. Smith, P. J. Strauss, and P. R. Levitt, [1994] Detection of gas in sandstone reservoirs using AVO analysis: A 3D seismic case history using the Geostack technique: *Geophysics*, **59**, 1362–1376.
- Lüning, S. and S. Kolonic, [2003] Uranium spectral gamma-ray response as a proxy for organic richness in black shales: applicability and limitations, *J. of Pet. Geol.*, **26**, 153–174.
- Mazumdar, P., [2007] Poisson dampening factor: *The Leading Edge*, **26**, 850–852, doi:10.1190/1.2756862.
- McMillan, J.M., L. J. Knapp, and N.B. Harris, [2014] Mineralogical Characterization of the Upper Devonian Duvernay Formation of Alberta, Western Canada Sedimentary Basin, *CSEG GeoConvention*, Expanded Abstracts.
- Mendelson, J. D. and M. N. Toksöz, [1985] Source rock characterization using multivariate analysis of log data, *SPWLA Twenty-sixth Ann. Logging Symposium*, 1–21.
- Passey, Q. R., S. Creaney, J. B. Kulla, F. J. Moretti, and J. D. Stroud, [1990], A practical model for organic richness from porosity and resistivity logs: *AAPG Bulletin*, **74**, no. 12, 1777–1794.
- Puryear, C.I. and J. P. Castagna, [2008] Layer-thickness determination and stratigraphic interpretation using spectral inversion: theory and application. *Geophysics*, **73**, R37–R48.
- Quakenbush, M., B. Shang, and C. Tuttle, [2006] Poisson impedance: *The Leading Edge*, **25**, 128–138, doi:10.1190/1.2172301.
- Rivard, C., D. Lavoie, R. Lefebvre, S. Sejourne, C. Lamontagne, and M. Duchesne, [2013] An overview of Canadian shale gas production and environmental concerns. *Internal journal of coal geology*. <http://dx.doi.org/10.1016/j.coal.2013.12.004>.
- Rokosh, C.D., S. Lyster, S.D.A. Anderson, A.P. Beaton, H. Berhane, T. Brazzoni, D. Chen, Y. Cheng, T. Mack, C. Pana and J. G. Pawlowicz, [2012] Summary of Alberta's Shale- and Siltstone-Hosted Hydrocarbons, *Energy Resources Conservation Board October Report*.
- Sharma, R. K. and S. Chopra, [2013] Unconventional reservoir characterization using conventional tools: 83rd Annual International Meeting, *SEG, Expanded Abstracts*, 2264–2268.
- Sharma, R. K. and S. Chopra, [2015] Determination of lithology and brittleness of rocks with a new attribute, *The Leading Edge*, **34**(5), 936–941.
- Whitcombe, D., [2002] Elastic impedance normalization, *Geophysics*, **67**, 60–62.
- Whitcombe, D. N., P. A. Connolly, R. L. Reagan and T. C. Redshaw, [2002] Extended elastic impedance for fluid and lithology prediction, *Geophysics*, **67**(1), 63 – 67.

EAGEEUROPEAN
ASSOCIATION OF
GEOSCIENTISTS &
ENGINEERSThe National
IOR Centre
of NorwayS
University of
Stavanger

IRIS

IFE



Sustainable IOR in a Low Oil Price World

Submit your abstract now!
Deadline 15 September 201619TH EUROPEAN SYMPOSIUM ON IMPROVED OIL RECOVERY
STAVANGER, NORWAY | 24-27 APRIL 2017